EurJIC European Journal of Inorganic Chemistry
ChemPubSoc Europe
FULL PAPER

DOI:10.1002/ejic.201402610

Preparation of Alginate/Graphene Oxide Hybrid Films and Their Integration in Triboelectric Generators

Luca Valentini,*[a] Nicoletta Rescignano,[b] Debora Puglia,[a] Marta Cardinali,[a] and Josè Kenny[a,b]

Keywords: Nanostructures / Organic-inorganic composites / Thin films / Energy conversion / Graphene / Carbohydrates

Sodium alginate/graphene oxide (Al/GO) nanocomposite films were prepared by solvent casting. The structure, morphology, and electrical properties of Al/GO films were characterized by Fourier transform infrared spectroscopy, Raman spectroscopy, scanning electron microscopy, and thermal analysis. The utilization of such an Al/GO film for a device that uses friction as the charging process to convert mechanical energy into electric power is reported. The triboelectric generator (TEG) was fabricated by stacking a drop-cast Al/GO film bewteen indium–tin oxide (ITO)-coated poly(ethylene terephthalate) (PET) and a PET sheet. Furthermore, the utilization of such a TEG as a pressure sensor is also illustrated.

Introduction

Alginate (Al) is a water-soluble polysaccharide that is isolated from brown algal species. Alginates are biodegradable, biocompatible, and nontoxic.[1,2]

Because of its reversible solubility, alginate can be fabricated in various forms, such as films, microspheres, and fibers.[3–5] Over the last two decades, alginate fibers have become well established in the wound-treatment industry,[6,7] in which their ion-exchange and gel-forming abilities are particularly useful for the treatment of exuding wounds.

Despite this, alginates still display some unsatisfactory properties such as low mechanical strength. Modification of alginates with inorganic materials is another way to improve alginate properties such as mechanical strength.[8–10]

Graphene, a one-atom-thick layer made of sp^2-hybridized carbon atoms obtained for the first time in 2004,[11] can be formally considered the basic building block of all sp^2-carbon allotropes including carbon nanotubes.

Numerous strategies for the preparation of homogeneously dispersed graphene–polymer composites have already been presented for a variety of advanced polymer matrices,[12,13] but there is a general agreement that a lot of research has to be dedicated to the development of easy and cost-effective methodologies towards the large-scale application of graphene in functional polymer composite materials for technological uses, such as biosensors, energy storage, and electronic devices.

[a] Department of Civil and Environmental Engineering, University of Perugia, Strada di Pentima 4, 05100 Terni, Italy
E-mail: luca.valentini@unipg.it
http://www.unipg.it/materials
[b] Institute of Polymer Science and Technology, CSIC, Juan de la Cierva 3, 28006 Madrid, Spain

The graphite exfoliation into graphene oxide (GO) sheets, which are easily processable in both aqueous and organic media as single-layer sheets,[14–16] is an alternative route to obtaining larger and soluble graphene quantities. Nanocomposites have been created with GO and water-soluble polysaccharides such as alginates.[17]

The presence of hydrophilic organic functional groups facilitates exfoliation and dispersion of GO in aqueous solution, but the material shows insulating properties because of the numerous defects that disrupt the sp^2 structure.

Materials that usually are less conductive or insulators when coming into contact with each other and then separated gives rise to the well-known effect called triboelectric charging. It is worth noting that the insulating property of some polymer nanocomposites allows for a long-time retention of triboelectric charges.[18]

The first attempt to create flexible triboelectric generators (TEG) was reported by Wang et al.[19] The same authors reported the first self-powered pressure sensors based on TEGs.[20]

The general physical process for energy conversion involves three steps: charge generation, charge separation, and charge flow. In piezoelectric nanogenerators the piezoelectric potential is created under mechanical strain. Recently, flexible triboelectric generators using all-polymer-based materials have been developed.[20,21]

They work in different modes: sliding mode and contact mode. For the sliding mode,[20] the potential difference is created by the horizontal in-plane separation of tribo-charged layers, whereas for contact mode,[22] the potential difference (polarization) is induced by the vertical out-of-plane separation of the tribo-charged layers.

The chemical groups of GO have been found to improve interfacial interaction between graphene oxide and the al-

© 0000 Wiley-VCH Verlag GmbH & Co. KGaA, Weinheim

ginate and pave the way for developing GO-based nanocomposites with remarkable mechanical and thermal properties.[8–10]

In this paper, we present a triboelectric generator based on biodegradable Al/GO film stacked between an indium–tin oxide (ITO) electrode and a poly(ethylene terephthalate) sheet. It was observed that if the two surfaces are rubbed against each other, a flow of electric charges across an external load was generated. In particular, the fabricated triboelectric generator can produce a short-circuit current density. Moreover, the fabricated device has been utilized in sensing by recording the output current signal under pressure. This work represents, to the best of our knowledge, the first example of the practical application of polysaccharides in energy harvesting and self-powered sensor systems.

Results and Discussion

When working on the laboratory scale, the solution-casting technique for the preparation of Al/GO always gives rise to highly homogeneous, flexible films with an average thickness of approximately 300–400 µm, as represented in Figure 1 (a).

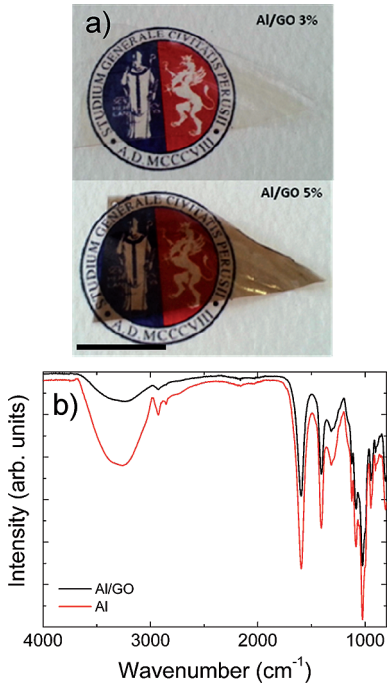

Figure 1. (a) Photograph (scale bar indicates 1 cm) of Al/GO films, and (b) FTIR spectra of Al and Al/GO films.

FTIR analysis was carried out to investigate the interaction between GO and Al as reported in Figure 1 (b). In the Al spectrum, the peak at 3347 cm^{-1} is attributed to an OH stretching vibration, the bands at 1600 and 1414 cm^{-1} correspond to the symmetric and asymmetric COO– stretching vibration of the carboxylate salt group; and the peak at 1030 cm^{-1} is assigned to the stretching vibration of C–O–C groups, respectively.[23] The FTIR spectrum of GO and Al were similar to those previously presented in the literature.[17,24]

Moreover, with the addition of GO, the peak at 3347 cm^{-1} (O–H stretching vibration) broadens and shifts to smaller wavelengths (3331 cm^{-1}), which can be attributed to the interaction of Al and GO through intermolecular hydrogen bonds.[17]

The XRD pattern (Figure 2, a) of Al film shows a broad diffraction peak at about 13.32° with an average intermolecular distance of 6.63 Å, thus indicating a rather amorphous structure.[25]

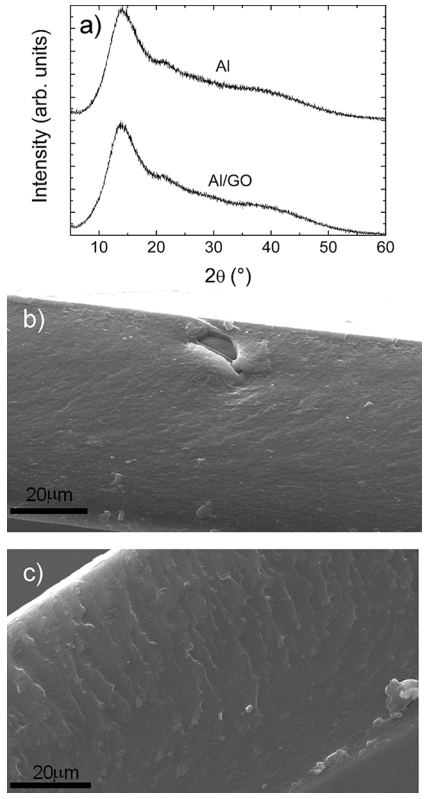

Figure 2. (a) XRD patterns of Al and Al/GO films. FESEM images of (b) Al and (c) Al/GO films.

The Al structure was not significantly affected by the incorporation of GO, which indicated that there were mainly physical interactions between Al and GO.[26]

On the basis of FESEM micrographs, the cross-section of the Al film displays a homogeneous morphology (Figure 2, b). The composite film (Figure 2, c) revealed a rather rough morphology, which might be attributed to the GO sheets embedded in the Al matrix.

The degree of exfoliation of the initial graphite flakes was also investigated with Raman spectroscopy characterization. Indeed, Raman spectroscopy allows the unambiguous nondestructive identification of single-layer, bilayer, and few-layer graphene flakes.[27]

A representative Raman spectrum of the GO relative to that of Al/GO sample is shown in Figure 3. The presence of the main peaks of GO[27] is clearly evident: the G band at approximately 1570 cm^{-1}, the 2D band at approximately

 © 0000 Wiley-VCH Verlag GmbH & Co. KGaA, Weinheim

2700 cm^{-1}, and the disorder-related D peak at approximately 1350 cm^{-1}.

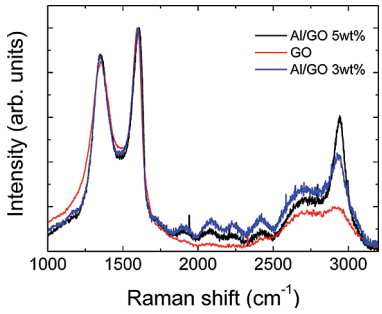

Figure 3. Raman spectra of GO and Al/GO films with 3 and 5 wt.-% of GO, respectively.

The G peak corresponds to the E_{2g} phonon at the Brillouin zone center. The D peak is due to breathing modes of sp^2 rings and requires a defect for its activation by double resonance.[27,28] The 2D peak is the second order of the D peak.

The Raman spectrum of the Al/GO sample shows a significant change in the shape of the 2D band signal; in addition to the G and D peaks, the 2D peak has a significant combination mode D + D′ at approximately 2940 cm^{-1}. The 2D peak thus consists of two components at 2700 and (D + D′) at 2940 cm^{-1}. According to what was found in the FTIR analysis and reported in the literature,[27] these data confirm the obtainment of an exfoliation of the GO sheets in the alginate matrix. In particular, the relative intensity of the D + D′ peak was found to increase by increasing the amount of GO up to 5% in the 5% Al matrix. This finding suggests that the best exfoliation for GO was obtained for such composite film.

The thermal properties of the composite films were evaluated with thermogravimetric analysis (TGA) and differential scanning calorimetry (DSC). TGA reveals the composition and changes in the thermal stability of the tested samples. Because both Al/GO films are mainly composed of alginate, their TGA curves are similar to that of the pristine alginate. In the thermograms (Figure 4, a) the alginate undergoes two-stage thermal degradation processes in which the first stage is attributed to the loss of volatile products through dehydration, whereas the weight loss in the second stage (two overlapping steps) is attributed to the degradation of the polymer and the formation of a carbonaceous residue.[29] In the case of Al/GO films, no substantial differences were detected in terms of thermal stability of the films; indeed, only a different residue at the end of the test was measured owing to the presence of the GO. The dehydration was also evidenced by an endothermic peak close to 100 °C detected in DSC (Figure 4, b) during the first heating scan. After that, the decomposition of the biopolymer took place. It was shown that, in the presence of GO, the evaporation took place at different temperatures. Moreover, a different value for the reaction heat was measured, thus indicating a different water absorption capability modified by the hydrophilic GO even at low content.[30]

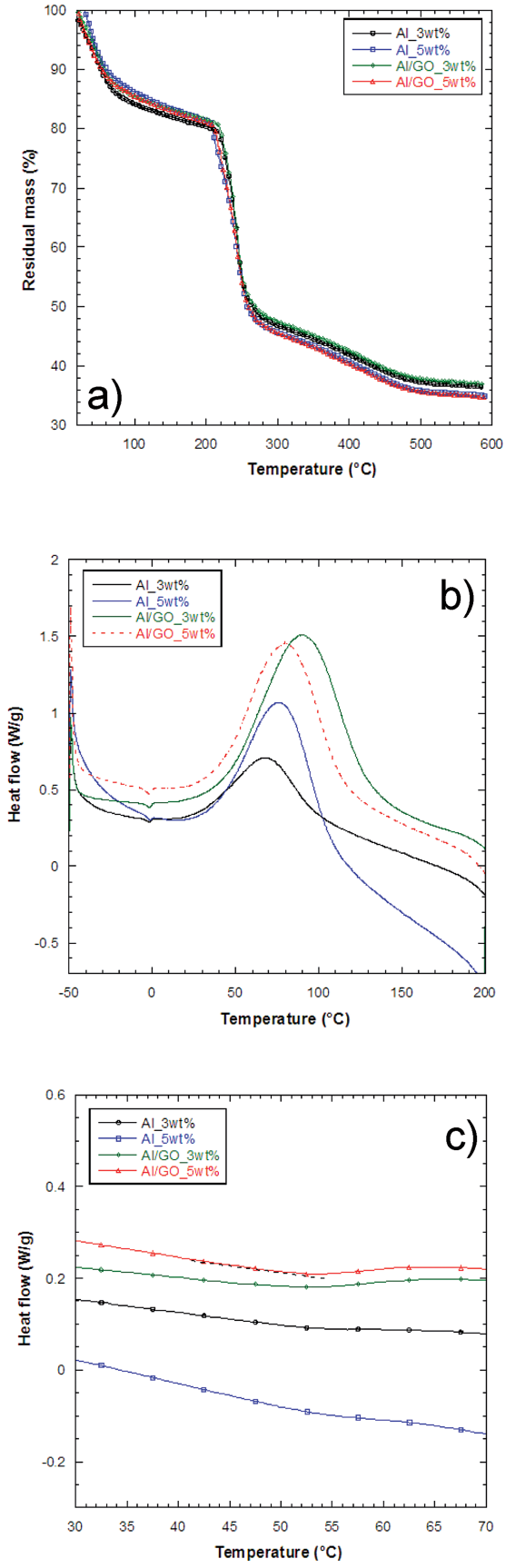

Figure 4. (a) TG curves for neat alginate and Al/GO films. (b) DSC first heating and (c) second heating scan for neat alginate and Al/GO films.

 © 0000 Wiley-VCH Verlag GmbH & Co. KGaA, Weinheim

Moreover, the heat-flow curves registered during the second heating scan (Figure 4, c) confirmed a constant value for the glass transition temperature of the alginate (nearly 58 °C), which remains unchanged even in the presence of the graphene oxide.

Synthetic and bioderived polymers that contain carboxy groups, such as polyacrylic acid and carboxymethyl cellulose, are generally used as polymer binders for porous composites used in energy-storage devices, such as electrodes in primary and secondary batteries, double-layer capacitors, electrochemical capacitors, supercapacitors, and electrochemical capacitor/battery hybrid devices.[31]

The molecular architecture of alginates has been optimized to facilitate the growth and survival of brown algae and many microorganisms in strong electrolyte environments, which is desirable for energy-storage devices. Therefore such bioderived active materials show great promise for energy-harvesting applications.

Alginate, unlike many polysaccharides commonly found in terrestrial plants, contains carboxylic groups at each monomeric unit of the polymer. This high content of carboxylic groups is desirable because carboxylic groups readily form rigid hydrogen bonds with oxidized surfaces, which enhances the stability and mechanical strength of energy-storage device components, for example, electrodes. Moreover alginate easily dissolves in water. This solubility characteristic lowers manufacturing costs, simplifies processing steps, and makes alginate more environmentally friendly than other binders.

The carboxy groups in alginate bind well to materials used as current collectors (for example, anodes and cathodes made of C) and provide stability and high Coulombic efficiency during charging and discharging cycles.

The operating principle of the TEG for the case of dielectric-to-dielectric in contact mode can be described by the coupling of contact charging and electrostatic induction. There are insulating materials that have the tendency to gain or lose charges, thereby resulting in net negative charges and net positive charges at the opposite surfaces, respectively (Table 1). It is worth noting that the insulating property of the neat polymer and polymer composites allows such effect.

Table 1. Surface resistivity of the prepared samples.

Sample	Surface resistivity [$\Omega\,sq^{-1}$]
Al 3 wt.-%	3.5×10^{-8}
Al 5 wt.-%	9.5×10^{-7}
Al/GO 3 wt.-%	4.1×10^{-7}
Al/GO 5 wt.-%	3.6×10^{-7}

Figure 5a shows the device layout of the fabricated TEG. Accordingly, to Wang et al.[32] the energy conversion consists of two major steps: (i) As the device was applied with an external compressive force, the two polymer layers are brought into contact and contact electrification occurs between the two layers. It should be noted that in this initial

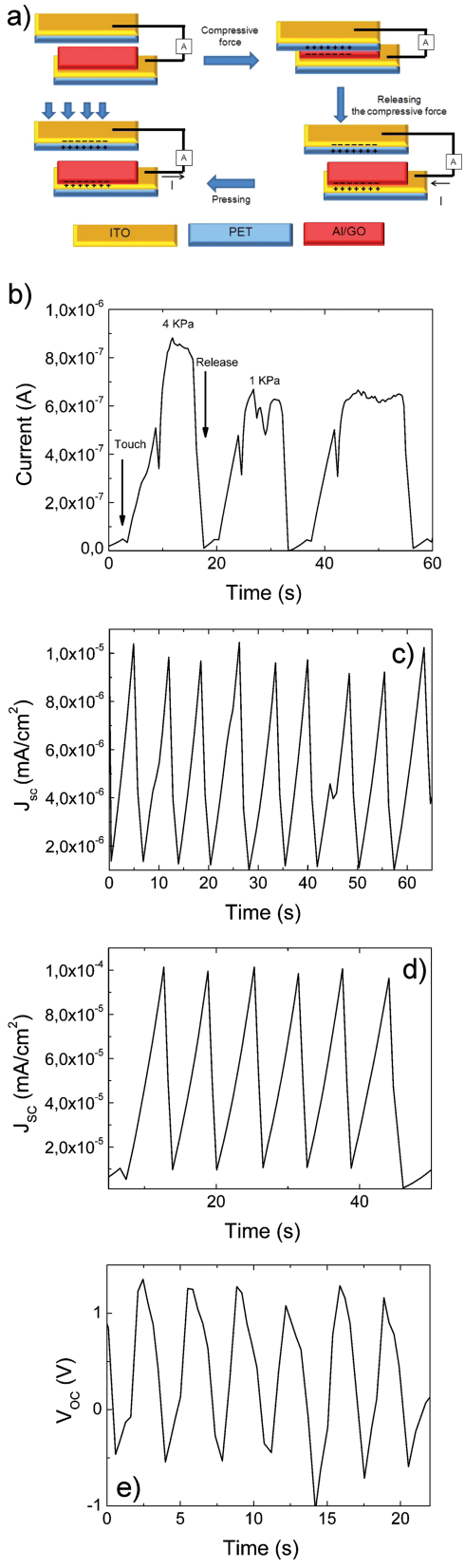

Figure 5. (a) Proposed mechanism of the TEG device. (b) Electrical current of the TEG device during touch and release cycles. Short-circuit current density signals of composite films with (c) 3 wt.-% and (d) 5 wt.-% of GO under various bending cycles (strain 0.2%) at about 0.15 Hz. (e) Open-circuit voltage of the composite film with 5 wt.-% of GO.

 © 0000 Wiley-VCH Verlag GmbH & Co. KGaA, Weinheim

step there will be no charge induction in the external load, since the two layers are strongly attached to each other with no separation of charges. (ii) With the release of the compressive force, an air gap will exist between the tribo-charged layers owing to the elastic resilience of the materials, thus introducing charge separation between the tribo charges and hence the potential difference between the top and bottom electrodes, which will serve as the driving force for the electron flow in the external load.

The fabricated device was loaded with different pressures and the corresponding output current signal was observed, as illustrated in Figure 5 (b). When the applied pressure on the Al/GO sample was released, a recovery of the current signal was observed.

Figure 5 (c and d) show the output performance of the TEG devices fabricated with GO content of 3 and 5 wt.-%, respectively. The TEG device fabricated with the highest GO content produces a short-circuit current density of 1×10^{-4} mA cm^{-2} with an open-circuit voltage up to 1.3 V (Figure 5, e). This result corresponds to a peak power density of 1.33 mW m^{-2}. With respect to the state of the art, the obtained results are far from the output power density obtained from nanostructured TEG.[33–35] This study is an early-stage proof of concept for the potential application of such materials for a self-powered bioelectronic device.

Conclusion

Alginate/GO nanocomposite films have been successfully prepared using a simple solution-casting method. FTIR and Raman spectroscopic results suggested that GO sheets form an interaction with the Al matrix and that GO undergoes exfoliation within the Al matrix, respectively. In addition, FESEM analysis demonstrated that such a method results in a uniform distribution of GO sheets within the Al matrix. We report then a triboelectric generator based on such composite films. A fabrication process based on inexpensive raw materials or expensive techniques is also reported. Alginate/GO-based TEGs exhibit energy harvesting from mechanical deformation and potential applications in pressure sensor systems.

Experimental Section

Layered graphene oxide made by a modified Hummers method was purchased from CheapTubes, USA. Alginic acid sodium salt from brown algae was purchased from Sigma–Aldrich. The films were prepared with different concentrations of graphene oxide using the solvent-casting method. The alginate solution was obtained by dissolving the sodium alginate in double-distilled (DD) water as a 3 and 5% (w/v) solution. Composite films with different GO contents (3 and 5 wt.-%) were produced by dropwise addition of a GO suspension to the sodium alginate solution. The resulting mixture was constantly stirred for about 30 min using a magnetic stirrer. Each solution was cast onto a transparent glass Petri dish and left for 72 h at 37 °C to allow the formation of a thin film. By using such a solvent-casting technique, Al/GO films were fabricated with a thickness of about 300–400 μm.

Thermal properties of the films were investigated by means of DSC (Mettler Toledo 822e) and TGA analysis (Seiko Exstar 6300). In detail, a heating scan from room temperature (up to 600 °C) under an inert atmosphere (50 mL min^{-1}) at 10 °C min^{-1} was performed for the TGA test, whereas the DSC tests were carried out by performing a heating/cooling/heating cycle at 10 °C min^{-1} from –50 up to 200 °C at 10 °C min^{-1}.

Raman measurements were obtained with a Renishaw InVia Reflex Raman system (Renishaw plc., Wotton-under-Edge, UK) by using a grating spectrometer with a Peltier-cooled charge-coupled device (CCD) detector coupled to a confocal microscope. All spectra were processed with Renishaw WiRE 3.2 software. The Raman scattering was excited by using an argon-ion laser wavelength of 514.5 nm. The laser beam was focused on the sample with a 50× microscope objective (numerical aperture = 0.75), with a laser power at the sample of around 2 mW. FTIR spectra were performed with a Perkin–Elmer Spectrum One FTIR spectrometer equipped with an ATR accessory. Spectra were recorded in the range of 650–4000 cm^{-1} with a resolution of 1 cm and an accumulation of 16 scans. Wide-angle X-ray spectroscopy (WAXS) was performed with a Bruker D8 Advance with a parallel Göbel mirror and a Vantec PSD detector with an applied voltage of 40 kV, an intensity of 40 mA, and by using a Cu-K_α (λ = 0.15418 nm) source. The samples were scanned from 5 to 60° (2Θ range).

Freeze-dried samples were fractured and coated with gold, then the surface morphology was observed with a Philips XL-30 FESEM. The electrical conductivity of the samples was measured with a Keithley 6517B electrometer/high-resistivity meter together with a Keithley 8089 resistivity test fixture. By using this test fixture, surface resistivity in the range of 10^3–10^{17} Ω could be measured.

The triboelectric generator was prepared by fixing the alginate/graphene oxide film onto ITO-coated poly(ethylene terephthalate) (ITO/PET) substrate (Sigma Aldrich, Milan, Italy; surface resistivity 45 Ω per square, dimensions of 4 cm × 1 cm × 1 mm, transmittance > 79% at 550 nm). The thickness of the alginate/GO film was approximately 350 μm. The alginate/GO film was sandwiched between a bottom ITO-coated PET sheet and a top PET side; the ITO side of the top sheet was used for the electrical contact (see Figure 5, a). The two short edges of the device were sealed with adhesive tape to ensure adequate contact between the alginate/GO layer and the PET sheet. The top and bottom ITO films were used to extract an equal and opposite charge signal produced by friction at the interfacial region and serve as electrodes for connecting the device to an external circuit.

For the pressure sensor system, the TEG was loaded (up to 1 g, contact area 2 mm^2), and when the load was placed and removed, the output current was recorded with a Keithley 4200-SCS semiconductor analyzer. The output current was recorded by applying a bias voltage of 1 V.

For the measurement of the triboelectrical output of the device, an external force was applied to create device bending (strain 0.2% at about 0.15 Hz) by a mechanical motor, and there was friction between the Al/GO film and top PET layer, thereby resulting in the triboelectric potential and electrical output in the external circuit. The short-circuit current density values were monitored with a computer-controlled Keithley 4200 Source Measure Unit.

Acknowledgments

N. R. thanks the European project Genis Lab for the financial support.

 © 0000 Wiley-VCH Verlag GmbH & Co. KGaA, Weinheim

[1] B. H. A. Rehm, *Alginates: Biology and Application*, vol. 13, Springer, Berlin, **2009**.
[2] A. D. Augst, H. J. Kong, D. J. Mooney, *Macromol. Biosci.* **2006**, *6*, 623–633.
[3] M. Bogun, T. Mikolajczyk, S. Rabiej, *J. Appl. Polym. Sci.* **2009**, *114*, 70–82.
[4] Z. F. Dong, Q. Wang, Y. M. Du, *J. Membr. Sci.* **2006**, *280*, 37–44.
[5] A. Watthanaphanit, P. Supaphol, H. Tamura, S. Tokura, R. Rujiravanit, *Carbohydr. Polym.* **2010**, *79*, 738–746.
[6] Y. M. Qin, H. Q. Hu, A. X. Luo, *J. Appl. Polym. Sci.* **2006**, *101*, 4216–4221.
[7] Y. M. Qin, *Polym. Int.* **2008**, *57*, 171–180.
[8] M. Yadav, K. Y. Rhee, S. J. Park, *Carbohydr. Polym.* **2014**, *110*, 18–25.
[9] J. Fan, Z. Shi, M. Lian, H. Li, J. Yin, *J. Mater. Chem. A* **2013**, *1*, 7433–7443.
[10] Y. He, N. Zhang, Q. Gong, H. Qiu, W. Wang, Y. Liu, J. Gao, *Carbohydr. Polym.* **2012**, *88*, 1100–1108.
[11] K. S. Novoselov, A. K. Geim, S. V. Morozov, D. Jiang, Y. Zhang, S. V. Dubonos, *Science* **2004**, *306*, 666–669.
[12] Z. Xu, C. Gao, *Macromolecules* **2010**, *43*, 6716–6723.
[13] P. Fabbri, E. Bassoli, S. Bittolo Bon, L. Valentini, *Polymer* **2012**, *53*, 897–902.
[14] W. Gao, L. B. Alemany, L. Ci, P. M. Ajayan, *Nat. Chem.* **2009**, *1*, 403–408.
[15] D. Li, M. B. Mueller, S. Gilje, R. B. Kaner, G. G. Wallace, *Nat. Nanotechnol.* **2008**, *3*, 101–105.
[16] J. I. Paredes, S. Villar-Rodil, M. J. Fernandez-Merino, L. Guardia, A. Martinez-Alonso, J. M. D. Tascon, *J. Mater. Chem.* **2011**, *21*, 298–306.
[17] M. Ionita, M. A. Pandele, H. Iovu, *Carbohydr. Polym.* **2013**, *94*, 339–344.
[18] E. Németh, G. Schubert, A. Augsburg, V. Albrecht, *J. Electrost.* **2003**, *58*, 3–16.
[19] F.-R. Fan, Z.-Q. Tian, Z. L. Wang, *Nano Energy* **2012**, *1*, 328–334.
[20] F.-R. Fan, L. Lin, G. Zhu, W. Wu, R. Zhang, Z. L. Wang, *Nano Lett.* **2012**, *12*, 3109–3114.
[21] S. Wang, L. Lin, Y. Xie, Q. Jing, S. Niu, Z. L. Wang, *Nano Lett.* **2013**, *13*, 2226–2233.
[22] G. Zhu, C. Pan, W. Guo, C.-Y. Chen, Y. Zhou, R. Yu, Z. L. Wang, *Nano Lett.* **2012**, *12*, 4960–4965.
[23] V. K. Malesu, D. Sahoo, P. L. Nayak, *Int. J. Appl. Biol. Pharm. Technol.* **2011**, *2*, 402–411.
[24] L. Li, C. Li, J. Qiong, X. Pengfei, L. Xiaoting, Z. Qiuping, *Talanta* **2012**, *93*, 350–357.
[25] S. G. Kim, G. T. Lim, J. Jegal, K. J. Lee, *J. Membr. Sci.* **2000**, *174*, 1–15.
[26] D. Han, L. Yan, W. Chen, W. Li, *Carbohydr. Polym.* **2011**, *83*, 653–658.
[27] A. C. Ferrari, J. C. Meyer, V. Scardaci, C. Casiraghi, M. Lazzeri, F. Mauri, *Phys. Rev. Lett.* **2006**, *97*, 187401–187403.
[28] F. Tuinstra, J. L. Koenig, *J. Chem. Phys.* **1970**, *53*, 1126–1129.
[29] T. M. Mruthyunjaya Swamy, B. Ramaraj, J. H. Lee, *J. Appl. Polym. Sci.* **2008**, *109*, 4075–4081.
[30] G. Wang, B. Wang, J. Park, J. Yang, X. Shen, J. Yao, *Carbon* **2009**, *47*, 68–72.
[31] Z. Zhang, W. Bao, H. Lu, M. Jia, K. Xie, Y. Lai, J. Li, *ECS Electrochem. Lett.* **2012**, *1*, A34–A37.
[32] Y. Yang, H. Zhang, Z.-H. Lin, Y. S. Zhou, Q. Jing, Y. Su, J. Yang, J. Chen, C. Hu, Z. L. Wang, *ACS Nano* **2013**, *10*, 9213–9222.
[33] L. Lin, S. H. Wang, Y. N. Xie, Q. S. Jing, S. M. Niu, Y. F. Hu, Z. L. Wang, *Nano Lett.* **2013**, *13*, 2916–2923.
[34] Y. Yang, H. L. Zhang, J. Chen, Q. Jing, Y. S. Zhou, X. N. Wen, Z. L. Wang, *ACS Nano* **2013**, *7*, 7342–7351.
[35] P. Bai, G. Zhu, Y. Liu, J. Chen, Q. S. Jing, W. Q. Yang, J. S. Ma, G. Zhang, Z. L. Wang, *ACS Nano* **2013**, *7*, 6261–6266.

Received: June 30, 2014
Published Online: ■

 © 0000 Wiley-VCH Verlag GmbH & Co. KGaA, Weinheim

Nanocomposite Films

L. Valentini,* N. Rescignano, D. Puglia, M. Cardinali, J. Kenny **1–7**

Preparation of Alginate/Graphene Oxide Hybrid Films and Their Integration in Triboelectric Generators

Keywords: Nanostructures / Organic-inorganic composites / Thin films / Energy conversion / Graphene / Carbohydrates

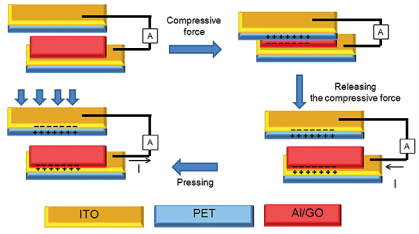

Sodium alginate/graphene oxide nanocomposite films were prepared by a solvent-casting method. We report the proof of concept that such a hybrid system can be used as the active component of a triboelectric generator. The involvement of a biodegradable polymer might introduce new applications in biodegradable/biocompatible electronics.

 © 0000 Wiley-VCH Verlag GmbH & Co. KGaA, Weinheim